

# AHMF: Adaptive Hybrid-Memory-Fusion Model for Driver Attention Prediction

Dongyang Xu<sup>1</sup>, Qingfan Wang<sup>1\*</sup>, Ji Ma<sup>2</sup>, Xiangyun Zeng<sup>3</sup>, and Lei Chen<sup>3</sup>

<sup>1</sup> School of Vehicle and Mobility, Tsinghua University

<sup>2</sup> College of Engineering, Peking University

<sup>3</sup> SenseTime Research

{xudy22 wqf20}@mails.tsinghua.edu.cn

**Abstract.** Accurate driver attention prediction can serve as a critical reference for intelligent vehicles in understanding traffic scenes and making informed driving decisions. Though existing studies on driver attention prediction improved performance by incorporating advanced saliency detection techniques, they overlooked the opportunity to achieve human-inspired prediction by analyzing driving tasks from a cognitive science perspective. During driving, drivers’ working memory and long-term memory play crucial roles in scene comprehension and experience retrieval, respectively. Together, they form situational awareness, facilitating drivers to quickly understand the current traffic situation and make optimal decisions based on past driving experiences. To explicitly integrate these two types of memory, this paper proposes an Adaptive Hybrid-Memory-Fusion (AHMF) driver attention prediction model to achieve more human-like predictions. Specifically, the model first encodes information about specific hazardous stimuli in the current scene to form working memories. Then, it adaptively retrieves similar situational experiences from the long-term memory for final prediction. Utilizing domain adaptation techniques, the model performs parallel training across multiple datasets, thereby enriching the accumulated driving experience within the long-term memory module. Compared to existing models, our model demonstrates significant improvements across various metrics on multiple public datasets, proving the effectiveness of integrating hybrid memories in driver attention prediction.

**Keywords:** Driver attention prediction · Long-term memory · Working memory · Transformer

## 1 Introduction

Human drivers primarily rely on visual information to drive. The distribution of their visual attention reflects experienced drivers’ cognitive understanding of

---

\* Corresponding author

D. Xu and Q. Wang — Equal contributions.

D. Xu — This work was done during the internship at SenseTime.

the current traffic scene, particularly in safety-critical scenarios with collision risks. For intelligent vehicles, accurately predicting driver attention is crucial for quickly identifying key risk elements in traffic scenes and assisting decision-making systems in making effective collision avoidance decisions [1, 2].

Due to such significant research significance, numerous studies on driver attention prediction have emerged [3–6]. These studies typically adopted the basic encoder-decoder model architecture, using CNN or Transformer as core components. However, current attention prediction models’ performance improvements are primarily attributed to backbone advancements in computer vision while neglecting the necessary cognitive mechanism analysis of the driving task itself. Consequently, these models have not yet achieved human-inspired driver attention prediction.

During driving, human drivers must process complex and variable traffic information in real time, especially in safety-critical scenarios. This cognitive process involves both working memory and long-term memory [7, 8]. The working memory module rapidly processes visual information by quickly identifying key risk objects in the current scene and assessing their danger [9]. When a potential collision is imminent, drivers rapidly retrieve relevant experiences from long-term memory. Together, these processes help drivers form situational awareness, quickly comprehend the current traffic situation, and make optimal decisions based on accumulated driving experience [9–12].

To achieve more human-like driver attention predictions, this paper proposes an Adaptive Hybrid-Memory-Fusion (AHMF) model by explicitly incorporating both working memory and long-term memory into driver attention prediction. Furthermore, leveraging domain adaptation, our model performs parallel training across multiple datasets, effectively enriching long-term memory with a diverse range of driving experiences. By combining specific dangerous stimuli in the scene (processed by the encoder as working memory) with retrieved experiences from the long-term memory, the model makes the final optimal predictions. We evaluated our model through comparative experiments on multiple public datasets. The results indicate that our model outperforms existing SOTA models across several metrics. The contributions of this paper are as follows:

1. We predict drivers’ visual attention in a manner that closely aligns with their understanding of traffic scenes from a cognitive science perspective. Specifically, the model first encodes specific dangerous stimuli in the current scene to form working memory, which is then integrated with long-term memory to produce the final scene encoding.
2. Utilizing domain adaptation, we achieve parallel training on multiple datasets, thereby enhancing the diversity of information in the long-term memory module and forming a comprehensive “driving experience” knowledge base, significantly boosting the model’s generalization capability.
3. Experiments demonstrate that our model achieves state-of-the-art prediction performance across several metrics on multiple public datasets.

## 2 Related Work

### 2.1 Driver Attention Prediction

The research on driver attention prediction has evolved through three stages: early machine learning methods, CNN-based methods, and Transformer-based methods. Initially, classical machine learning approaches, such as dynamic Bayesian models, adopted bottom-up and top-down frameworks to simulate drivers’ visual attention [13–15]. With the development of CNN, convolutional prediction methods became mainstream. These models typically employ an encoder-decoder structure, where encoders process current scene information while decoders reconstruct visual attention distributions [16–20]. Recently, the impressive performance of Transformers in computer vision has led to the development of Transformer-based image/video saliency detection [21–24]. Despite these advancements, these studies have not yet achieved human-inspired predictions, as they lack cognitive science insights into the driving task. Models that align more closely with human drivers’ scene understanding mechanisms are expected to enhance prediction accuracy further.

### 2.2 Memory-Augmented Deep Learning

The integrated development of cognitive science and deep learning has led to the birth of memory-augmented models that simulate external memory to overcome the limitations of working memory [25]. A notable early example is the Long Short-Term Memory (LSTM) model [26]. Subsequent deep learning models have explored various forms of external memory integration [27–31]. For driver attention prediction, FBLNet incorporates a feedback loop structure to achieve incremental knowledge, which can be seen as a kind of simple long-term memory [24]. Our approach differs by proposing staged modeling of working memory and long-term memory and an effective memory fusion fashion. Meanwhile, incorporating domain adaptation significantly enriched the accumulated “driving experience” in long-term memory, as well as a better generalization ability.

## 3 Method

In this section, we proposed a novel Adaptive Hybrid-Memory-Fusion (AHMF) driver attention prediction model that explicitly incorporated drivers’ both working memory and long-term memory to achieve human-like predictions. Fig. 1 illustrates the overview of AHMF, which involves two core modules, *i.e.*, temporal-spatial working memory encoding and attention-based hybrid memory fusion. In addition, necessary domain-specific modules were incorporated to enrich the accumulated long-term memory across various datasets. Given the length constraints of this paper, we will primarily use textual descriptions and avoid complex mathematical formulas to detail the proposed AHMF model.

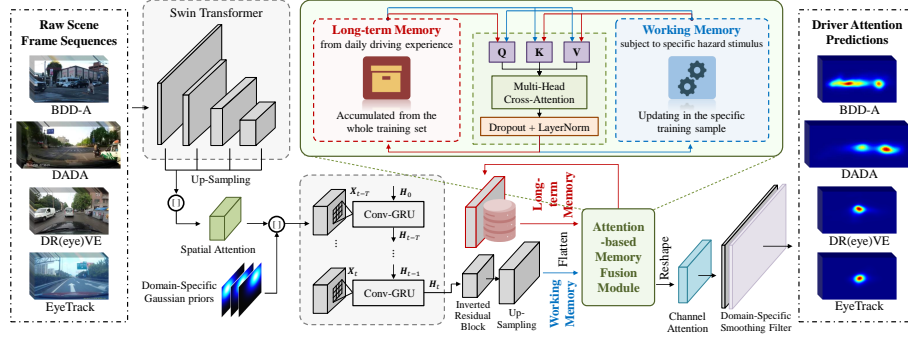


Fig. 1: Overview of the proposed AHMF driver attention prediction model.

### 3.1 Temporal-Spatial Working Memory Encoding

Complex traffic scenes, particularly safety-critical scenarios, display not only strong temporal correlation characteristics but also spatially unbalanced distributions of critical risk objects, both significantly affecting the encoding process of drivers' working memory. Thus, it is necessary to adopt the pattern of hybrid temporal-spatial encoding to achieve accurate driver attention prediction.

In terms of spatial encoding, we first adopted a Swin Transformer-tiny [32] as the backbone to extract essential semantic features. Extracted features at different levels were first normalized into the same dimension with up-sampling and then concatenated to capture semantic information in different ranges. Then, a spatial-attention-based convolution module was designed to model the inherent relationships over various local features of traffic frames, which has been proven effective in enhancing its spatial representation capability [12, 33]. The spatial attention module can be formulated as follows:

$$\mathbf{y}_i = \sum_{j=1}^{H \times W} (W_\omega \mathbf{x}_j) \frac{\exp(\mathbf{x}_i^T W_\theta^T \cdot W_\phi \mathbf{x}_j)}{\sum_{j=1}^{H \times W} \exp(\mathbf{x}_i^T W_\theta^T \cdot W_\phi \mathbf{x}_j)} \quad (1)$$

where  $x_i$  and  $y_i$  are the input and output pixel at the position index of  $i$ -th, respectively,  $i, j \in \mathbb{R}^{(H \times W)}$  denote the flattened  $1d$  position index of features along the spatial dimension, and the matrixes  $W_\theta$ ,  $W_\phi$ , and  $W_\omega$  represent the learnable parameters of  $1 \times 1$  convolution layers. Then, the encoded features were concatenated with predefined domain-specific Gaussian priors to enhance generalization ability in various heterogeneous driving scenes.

Regarding temporal encoding, we utilized convolutional gated recurrent units (Conv-GRUs) to realize the efficient transmission of temporal traffic information based on the update gate and reset gate [34, 35]. We selected Conv-GRUs instead of Conv-LSTM due to its lightweight network structure, which is more suitable for efficient online inference under safety-critical scenarios.

### 3.2 Attention-based Hybrid Memory Fusion

Human drivers’ working memory (for scene comprehension) and long-term memory (for experience retrieval) during driving were independently modeled in AHMF. Further, we designed an efficient adaptive memory fusion module using the attention mechanism, which was inspired by human drivers’ situational awareness mechanism.

**Working Memory Modeling.** Obtaining the temporal-spatial encoded features from the encoder, we used an inverted residual block [36] to reduce the channel dimension before adopting an up-sampling layer to adjust the spatial dimensions of features.

**Long-term Memory Modeling.** The long-term memory module was modeled as an offline knowledge base, and it was initialized as a set of learnable parameters with the same size as working memory (*i.e.*,  $H \times W \times C$ ). During training, it first retrieves critical driving experience according to the queries from working memory and is then updated to incorporate newly encoded features continuously.

**Attention-based Hybrid Memory Fusion.** We adopted two multi-head cross-attention-based fusion modules to facilitate the information transfer between two memories. Since attention modules take serialized data as inputs, working memory, and long-term memory were flattened at the spatial and channel dimensions.

First, to enhance the working memory with “driving experience” retrieved from long-term memories, we used linear layers to project working memory into queries and long-term memories into keys and values, respectively. A multi-head cross-attention module MHCA( $\cdot$ ) was adopted to model the inherent relationships between the two memories, developed as:

$$Q_w = \text{Linear}(m_w), \quad K_l = \text{Linear}(m_l), \quad V_l = \text{Linear}(m_l) \quad (2)$$

$$m_w^e = \text{MHCA}(q = Q_w + \text{PE}(Q_w), k = K_l + \text{PE}(K_l), v = V_l) \quad (3)$$

where  $m_w \in \mathbb{R}^{T \times (H \times W \times C)}$  and  $m_l \in \mathbb{R}^{T \times (H \times W \times C)}$  represent the working memories and long-term memories, respectively,  $m_w^e \in \mathbb{R}^{T \times H \times W \times C}$  denotes the enhanced working memories after reshaping to its original shape,  $T$  is the sequence length,  $H \times W \times C$  is the dimension of flattened features,  $q$ ,  $k$ , and  $v$  denote the query, key, and value in the multi-head cross-attention module, and  $\text{PE}(\cdot)$  denotes the sinusoidal position encoding of input tokens. Dropout and layer normalization were used after the cross-attention to stabilize the training process and avoid over-fitting.

Another multi-head cross-attention module with the switched keys, values (*i.e.*,  $K_w$  and  $V_w$  projected from working memory), and queries (*i.e.*,  $Q_l$  projected from long-term memories) was used to update the accumulated long-term memories (from  $m_l$  to  $m_l^e$ ) with the newly encoded working memory  $m_w^e$ . Long-term memories benefited from various driving experiences across multiple datasets. When used for online inference, the cross-attention module for updating long-term memories can be deprecated to accelerate inference time.

After memory fusion, a channel-attention-based convolution module enhanced the representation of high-level features across channels, formulated as:

$$\mathbf{y}_i = \sum_{j=1}^{H \times W} \frac{\exp(\mathbf{x}_i^T \cdot \mathbf{x}_j)}{\sum_{j=1}^{H \times W} \exp(\mathbf{x}_i^T \cdot \mathbf{x}_j)} (\mathbf{x}_j) \quad (4)$$

where dot-product similarity  $\mathbf{x}_i^T \cdot \mathbf{x}_j$  measures the mutual influences between  $i$ -th channel and  $j$ -th channel of input features. Finally, smoothing filters were used to blur final attention predictions.

### 3.3 Domain-Specific Modules for Domain Adaption

For better generalization ability, we also incorporated a series of domain adaptation techniques to perform parallel training across multiple datasets, which can further enrich the accumulated driving experience within the long-term memories. Following the previous studies on video saliency modeling [37, 38], three domain-specific modules were utilized in AHMF, including domain-specific batch normalization, domain-specific Gaussian priors, and domain-specific smoothing filters. **Domain-specific batch normalization** aims at reducing undesirable data heterogeneity across different datasets during batch normalization [39]. **Domain-specific Gaussian priors**, modeled by a series of learnable parameters, serve as vital spatial prior information for driver attention prediction for a specific dataset [40]. Considering the heterogeneous sharpness distributions of attention maps across datasets, we adopted **domain-specific smoothing filters** to blur final attention predictions to improve performance [38].

## 4 Experiments

In this section, we describe our experimental setup and compare the proposed AHMF model with several SOTA methods. For implementation details of AHMF, please refer to the supplementary material (S.1.1).

### 4.1 Experimental Settings

**Datasets.** The AHMF model was jointly trained and tested on four widely-used public large-scale driver attention datasets, *i.e.*, Driver Attention and Driver Accident (DADA) [41], Berkeley DeepDrive attention (BDD-A) [17], DReyeVE [42], and EyeTrack [19]. Detailed descriptions of these datasets can be seen in the supplementary material (S.1.2).

**Evaluation Metrics.** To comprehensively evaluate model performance, we adopt various saliency evaluation metrics, including three distribution-based metrics, *i.e.*, Similarity (SIM), Kullback-Leibler divergence (KLD), and Pearson’s correlation coefficient (CC), and two location-based metrics, *i.e.*, Normalized Scanpath Saliency (NSS) and Area Under ROC Curve Judd (AUC-J). Details are given in the supplementary material (S.1.3).

**Table 1:** Comparison of the AHMF model with state-of-the-art driver attention prediction models on the DADA and BDD-A datasets. Red values indicate the best performance, while blue values indicate the second-best.

Method	DADA [41]					BDD-A [17]				
	AUC-J $\uparrow$	SIM $\uparrow$	CC $\uparrow$	KLD $\downarrow$	NSS $\uparrow$	AUC-J $\uparrow$	SIM $\uparrow$	CC $\uparrow$	KLD $\downarrow$	NSS $\uparrow$
BDDA [17]	0.89	0.22	0.33	2.77	2.52	<b>0.93</b>	0.35	0.48	2.07	3.45
U2NET [43]	<b>0.94</b>	0.30	<b>0.47</b>	1.85	3.77	<b>0.95</b>	0.36	0.55	1.47	3.95
MINET [44]	0.86	0.30	0.38	9.99	3.62	0.86	0.35	0.48	10.5	4.28
DRIVER [45]	0.90	0.24	0.37	4.03	3.06	0.76	0.25	0.31	13.8	2.56
ADA [38]	<b>0.94</b>	0.36	<b>0.50</b>	<b>1.59</b>	3.51	0.92	<b>0.49</b>	<b>0.64</b>	<b>1.02</b>	4.56
DADA [41]	<b>0.95</b>	0.34	<b>0.47</b>	2.16	4.05	<b>0.95</b>	0.39	0.55	1.48	4.22
DBNET [6]	0.91	0.25	0.39	2.77	2.93	<b>0.95</b>	0.39	0.55	1.85	3.93
PGNet [21]	0.92	<b>0.37</b>	0.45	5.28	4.04	0.92	0.43	0.56	6.09	4.92
FBLNet [24]	<b>0.95</b>	0.33	<b>0.50</b>	1.92	<b>4.13</b>	<b>0.95</b>	0.46	<b>0.64</b>	1.40	<b>5.02</b>
<b>Ours</b>	<b>0.94</b>	<b>0.57</b>	<b>0.50</b>	<b>1.55</b>	<b>5.02</b>	0.92	<b>0.75</b>	<b>0.58</b>	<b>1.17</b>	<b>5.51</b>

## 4.2 Comparison with SOTA

**Quantitative Results.** Compared with several SOTA driver attention prediction models, our model demonstrates satisfying performance on both the DADA and BDD-A datasets (Table 4). Specifically, our model performs particularly well in SIM and NSS, achieving 0.57 and 5.02 on DADA and 0.75 and 5.51 on BDD-A, respectively, yielding a significant improvement of +54.0%, +21.5%, +53.1%, and +9.8% compared to the best existing methods. Additionally, our model achieves the lowest KLD of 1.55 and the highest CC of 0.50 on the DADA dataset. Furthermore, our model performs competitively in AUC-J and CC, closely matching the top-performing models. Overall, the AHMF model demonstrates significant advantages across multiple metrics, showing its robustness and effectiveness in driver attention modeling.

**Qualitative Results.** Figure 4 visualizes the comparison results of driver attention prediction. The MLNet model overly focuses on static areas in video frames, unlike human drivers who concentrate on objects with specific inter-frame changes. Similarly, PGNet not only pays too much attention to static regions but also fails to allocate attention to the road ahead in the absence of salient objects, dispersing attention to irrelevant areas such as roadside fences. In contrast, our model focuses on dynamic traffic participants with significant inter-frame changes, and its attention predictions align closely with the ground truth. More qualitative results can be found in the supplementary material (S.2.1).

## 4.3 Ablation Study

We now analyze several design choices for AHMF in a series of ablation studies on the DADA dataset.

Table 6 presents the results of an ablation study evaluating the contributions of different key components of our model. Specifically, it compares the



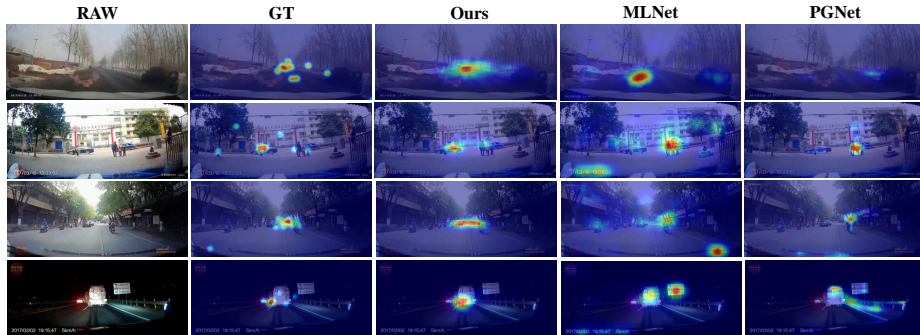


**Fig. 2:** Qualitative results of the predicted driver attention maps. From left to right: raw inputs, ground-truth maps, predictions of ours, MLNet [46], and PGNet [47].

**Table 2:** Ablation study for AHMF’s different components on the DADA dataset.

	AUC-J $\uparrow$	SIM $\uparrow$	CC $\uparrow$	KLD $\downarrow$	NSS $\uparrow$
w/o HMF	0.92	0.44	0.47	1.61	4.49
w/o SA	0.92	0.56	0.49	1.56	4.95
w/o CA	0.93	0.53	0.48	1.56	4.83
<b>w/ all</b>	<b>0.94</b>	<b>0.57</b>	<b>0.50</b>	<b>1.55</b>	<b>5.02</b>

**Table 3:** Ablation study for the duration of working memory on DADA.

	AUC-J $\uparrow$	SIM $\uparrow$	CC $\uparrow$	KLD $\downarrow$	NSS $\uparrow$
1.0 s	0.92	0.53	0.48	1.57	4.79
1.5 s	0.92	0.55	0.48	1.55	4.86
2.0 s	0.92	0.57	0.47	1.58	4.81
<b>3.0 s</b>	<b>0.94</b>	<b>0.57</b>	<b>0.50</b>	<b>1.55</b>	<b>5.02</b>

performance of the whole model against three variants: without the Hybrid-Memory-Fusion (HMF) module, without the Spatial-Attention (SA) module, and without the Channel-Attention (CA) module. The results indicate that removing any component results in decreased performance, demonstrating the critical importance of each component in achieving optimal performance. As expected, the introduction of the HMF module shows the most significant improvement, increasing SIM by +29.5% and NSS by +11.8%.

Table 7 analyzes the impacts of working memory durations in traffic scenes, *i.e.*, the length of historical input sequences. The results indicate that the shorter memory durations result in lower performance, particularly noticeable in the NSS metric. This demonstrates longer input sequences contribute to the temporal encoding of working memories and achieve more effective fusion of hybrid memories, finally enhancing driver attention predictions.

More detailed ablation experiments can be found in the supplementary material (S.2.2).

## 5 Conclusion

In this paper, we have presented a novel, more human-like driver attention prediction model that incorporates both working memory and long-term memory. Unlike the existing approaches, our method explicitly modeled human drivers’



working memory for scene comprehension and long-term memory for experience retrieval to imitate their situational awareness mechanism when locating their visual attention during driving. Experiments proved that the proposed method of memory modeling and fusion significantly contributed to the performance improvement of driver attention prediction. We modeled the two kinds of memories in a very straightforward way. More future efforts should be made to find a better method of memory modeling with a more in-depth interdisciplinary study between cognitive science and computer vision.

## References

1. Feiyan Hu, GM Venkatesh, Noel E O'Connor, Alan F Smeaton, and Suzanne Little. Utilising visual attention cues for vehicle detection and tracking. In *2020 25th International Conference on Pattern Recognition (ICPR)*, pages 5535–5542. IEEE, 2021. [2](#)
2. Muhammad Monjurul Karim, Yu Li, Ruwen Qin, and Zhaozheng Yin. A dynamic spatial-temporal attention network for early anticipation of traffic accidents. *IEEE Transactions on Intelligent Transportation Systems*, 23(7):9590–9600, 2022. [2](#)
3. Tao Deng, Lianfang Jiang, Yi Shi, Jiang Wu, Zhangbi Wu, Shun Yan, Xianshi Zhang, and Hongmei Yan. Driving visual saliency prediction of dynamic night scenes via a spatio-temporal dual-encoder network. *IEEE Transactions on Intelligent Transportation Systems*, 2023. [2](#)
4. Rui Fu, Tao Huang, Mingyue Li, Qinyu Sun, and Yunxing Chen. A multimodal deep neural network for prediction of the driver's focus of attention based on anthropomorphic attention mechanism and prior knowledge. *Expert Systems with Applications*, 214:119157, 2023. [2](#)
5. Ailiang Lin, Bingzhi Chen, Jiayu Xu, Zheng Zhang, Guangming Lu, and David Zhang. Ds-transunet: Dual swin transformer u-net for medical image segmentation. *IEEE Transactions on Instrumentation and Measurement*, 71:1–15, 2022. [2](#)
6. Han Tian, Tao Deng, and Hongmei Yan. Driving as well as on a sunny day? predicting driver's fixation in rainy weather conditions via a dual-branch visual model. *IEEE/CAA Journal of Automatica Sinica*, 9(7):1335–1338, 2022. [2](#), [7](#)
7. G Wood, G Hartley, PA Furley, and MR Wilson. Working memory capacity, visual attention and hazard perception in driving. *Journal of Applied Research in Memory and Cognition*, 5(4):454–462, 2016. [2](#)
8. David P Broadbent, Giorgia D'Innocenzo, Toby J Ellmers, Justin Parsler, Andre J Szameitat, and Daniel T Bishop. Cognitive load, working memory capacity and driving performance: A preliminary fairs and eye tracking study. *Transportation research part F: traffic psychology and behaviour*, 92:121–132, 2023. [2](#)
9. Huiming Zhang, Yingshi Guo, Wei Yuan, and Kunchen Li. On the importance of working memory in the driving safety field: a systematic review. *Accident Analysis & Prevention*, 187:107071, 2023. [2](#)
10. Josef F Krems and Martin RK Baumann. Driving and situation awareness: A cognitive model of memory-update processes. In *Human Centered Design: First International Conference, HCD 2009, Held as Part of HCI International 2009, San Diego, CA, USA, July 19-24, 2009 Proceedings 1*, pages 986–994. Springer, 2009. [2](#)
11. Joost CF De Winter, Yke Bauke Eisma, Christopher DD Cabrall, Peter A Hancock, and Neville A Stanton. Situation awareness based on eye movements in relation to the task environment. *Cognition, Technology & Work*, 21(1):99–111, 2019. [2](#)
12. Shun Gan, Quan Li, Qingfan Wang, WenTao Chen, Detong Qin, and Bingbing Nie. Constructing personalized situation awareness dataset for hazard perception, comprehension, projection, and action of drivers. In *2021 IEEE International Intelligent Transportation Systems Conference (ITSC)*, pages 1697–1704. IEEE, 2021. [2](#), [4](#)
13. Derek Pang, Akisato Kimura, Tatsuto Takeuchi, Junji Yamato, and Kunio Kashino. A stochastic model of selective visual attention with a dynamic bayesian network. In *2008 IEEE International Conference on Multimedia and Expo*, pages 1073–1076. IEEE, 2008. [3](#)

14. Martin Heracles, Gerhard Sagerer, Ursula Körner, Thomas Michalke, Jannik Fritsch, and Christian Goerick. A dynamic attention system that reorients to unexpected motion in real-world traffic environments. In *2009 IEEE/RSJ International Conference on Intelligent Robots and Systems*, pages 1735–1742. IEEE, 2009. [3](#)
15. Sang-Woo Ban, Bumhwi Kim, and Minho Lee. Top-down visual selective attention model combined with bottom-up saliency map for incremental object perception. In *The 2010 International Joint Conference on Neural Networks (IJCNN)*, pages 1–8. IEEE, 2010. [3](#)
16. Ashish Tawari and Byeongkeun Kang. A computational framework for driver’s visual attention using a fully convolutional architecture. In *2017 IEEE Intelligent Vehicles Symposium (IV)*, pages 887–894. IEEE, 2017. [3](#)
17. Ye Xia, Danqing Zhang, Jinkyu Kim, Ken Nakayama, Karl Zipser, and David Whitney. Predicting driver attention in critical situations. In *Computer Vision–ACCV 2018: 14th Asian Conference on Computer Vision, Perth, Australia, December 2–6, 2018, Revised Selected Papers, Part V 14*, pages 658–674. Springer, 2019. [3](#), [6](#), [7](#), [14](#), [17](#), [18](#)
18. Andrea Palazzi, Davide Abati, Francesco Solera, Rita Cucchiara, et al. Predicting the driver’s focus of attention: the dr (eye) ve project. *IEEE transactions on pattern analysis and machine intelligence*, 41(7):1720–1733, 2018. [3](#)
19. Tao Deng, Hongmei Yan, Long Qin, Thuyen Ngo, and BS Manjunath. How do drivers allocate their potential attention? driving fixation prediction via convolutional neural networks. *IEEE Transactions on Intelligent Transportation Systems*, 21(5):2146–2154, 2019. [3](#), [6](#), [14](#)
20. Tao Deng, Fei Yan, and Hongmei Yan. Driving video fixation prediction model via spatio-temporal networks and attention gates. In *2021 IEEE International Conference on Multimedia and Expo (ICME)*, pages 1–6. IEEE, 2021. [3](#)
21. Chenxi Xie, Changqun Xia, Mingcan Ma, Zhirui Zhao, Xiaowu Chen, and Jia Li. Pyramid grafting network for one-stage high resolution saliency detection. In *Proceedings of the IEEE/CVF conference on computer vision and pattern recognition*, pages 11717–11726, 2022. [3](#), [7](#)
22. Pin-Jie Huang, Chi-An Lu, and Kuan-Wen Chen. Temporally-aggregating multiple-discontinuous-image saliency prediction with transformer-based attention. In *2022 International Conference on Robotics and Automation (ICRA)*, pages 6571–6577. IEEE, 2022. [3](#)
23. Cheng Ma, Haowen Sun, Yongming Rao, Jie Zhou, and Jiwen Lu. Video saliency forecasting transformer. *IEEE Transactions on Circuits and Systems for Video Technology*, 32(10):6850–6862, 2022. [3](#)
24. Yilong Chen, Zhixiong Nan, and Tao Xiang. Fblnet: Feedback loop network for driver attention prediction. In *Proceedings of the IEEE/CVF International Conference on Computer Vision*, pages 13371–13380, 2023. [3](#), [7](#)
25. Hung Le. Memory and attention in deep learning. *arXiv preprint arXiv:2107.01390*, 2021. [3](#)
26. Sepp Hochreiter and Jürgen Schmidhuber. Long short-term memory. *Neural computation*, 9(8):1735–1780, 1997. [3](#)
27. David Lopez-Paz and Marc’Aurelio Ranzato. Gradient episodic memory for continual learning. *Advances in neural information processing systems*, 30, 2017. [3](#)
28. Aaditya Prakash, Siyuan Zhao, Sadid Hasan, Vivek Datla, Kathy Lee, Ashequl Qadir, Joey Liu, and Oladimeji Farri. Condensed memory networks for clinical diagnostic inferencing. In *Proceedings of the AAAI Conference on Artificial Intelligence*, volume 31, 2017. [3](#)

29. Jiyang Gao, Runzhou Ge, Kan Chen, and Ram Nevatia. Motion-appearance co-memory networks for video question answering. In *Proceedings of the IEEE conference on computer vision and pattern recognition*, pages 6576–6585, 2018. 3
30. Hung Le, Truyen Tran, and Svetha Venkatesh. Learning to remember more with less memorization. *arXiv preprint arXiv:1901.01347*, 2019. 3
31. Federico Landi, Lorenzo Baraldi, Marcella Cornia, and Rita Cucchiara. Working memory connections for lstm. *Neural Networks*, 144:334–341, 2021. 3
32. Ze Liu, Yutong Lin, Yue Cao, Han Hu, Yixuan Wei, Zheng Zhang, Stephen Lin, and Baining Guo. Swin transformer: Hierarchical vision transformer using shifted windows. In *Proceedings of the IEEE/CVF international conference on computer vision*, pages 10012–10022, 2021. 4
33. Sanghyun Woo, Jongchan Park, Joon-Young Lee, and In So Kweon. Cbam: Convolutional block attention module. In *Proceedings of the European conference on computer vision (ECCV)*, pages 3–19, 2018. 4
34. Xingjian Shi, Zhourong Chen, Hao Wang, Dit-Yan Yeung, Wai-Kin Wong, and Wang-chun Woo. Convolutional lstm network: A machine learning approach for precipitation nowcasting. *Advances in neural information processing systems*, 28, 2015. 4
35. Ziqi Zhang, David Robinson, and Jonathan Tepper. Detecting hate speech on twitter using a convolution-gru based deep neural network. In *The Semantic Web: 15th International Conference, ESWC 2018, Heraklion, Crete, Greece, June 3–7, 2018, Proceedings 15*, pages 745–760. Springer, 2018. 4
36. Mark Sandler, Andrew Howard, Menglong Zhu, Andrey Zhmoginov, and Liang-Chieh Chen. Mobilenetv2: Inverted residuals and linear bottlenecks. In *Proceedings of the IEEE conference on computer vision and pattern recognition*, pages 4510–4520, 2018. 5
37. Richard Droste, Jianbo Jiao, and J Alison Noble. Unified image and video saliency modeling. In *Computer Vision—ECCV 2020: 16th European Conference, Glasgow, UK, August 23–28, 2020, Proceedings, Part V 16*, pages 419–435. Springer, 2020. 6
38. Shun Gan, Xizhe Pei, Yulong Ge, Qingfan Wang, Shi Shang, Shengbo Eben Li, and Bingbing Nie. Multisource adaption for driver attention prediction in arbitrary driving scenes. *IEEE transactions on intelligent transportation systems*, 23(11):20912–20925, 2022. 6, 7, 14
39. Woong-Gi Chang, Tackgeun You, Seonguk Seo, Suha Kwak, and Bohyung Han. Domain-specific batch normalization for unsupervised domain adaptation. In *Proceedings of the IEEE/CVF conference on Computer Vision and Pattern Recognition*, pages 7354–7362, 2019. 6
40. Tao Deng, Kaifu Yang, Yongjie Li, and Hongmei Yan. Where does the driver look? top-down-based saliency detection in a traffic driving environment. *IEEE Transactions on Intelligent Transportation Systems*, 17(7):2051–2062, 2016. 6
41. Jianwu Fang, Dingxin Yan, Jiahuan Qiao, Jianru Xue, He Wang, and Sen Li. Dada-2000: Can driving accident be predicted by driver attentionf analyzed by a benchmark. In *2019 IEEE Intelligent Transportation Systems Conference (ITSC)*, pages 4303–4309. IEEE, 2019. 6, 7, 14, 17, 18
42. Stefano Alletto, Andrea Palazzi, Francesco Solera, Simone Calderara, and Rita Cucchiara. Dr (eye) ve: a dataset for attention-based tasks with applications to autonomous and assisted driving. In *Proceedings of the IEEE conference on computer vision and pattern recognition workshops*, pages 54–60, 2016. 6, 14

43. Xuebin Qin, Zichen Zhang, Chenyang Huang, Masood Dehghan, Osmar R Zaiane, and Martin Jagersand. U2-net: Going deeper with nested u-structure for salient object detection. *Pattern recognition*, 106:107404, 2020. 7
44. Youwei Pang, Xiaoqi Zhao, Lihe Zhang, and Huchuan Lu. Multi-scale interactive network for salient object detection. In *Proceedings of the IEEE/CVF conference on computer vision and pattern recognition*, pages 9413–9422, 2020. 7
45. Wentao Bao, Qi Yu, and Yu Kong. Drive: Deep reinforced accident anticipation with visual explanation. In *Proceedings of the IEEE/CVF International Conference on Computer Vision*, pages 7619–7628, 2021. 7
46. Marcella Cornia, Lorenzo Baraldi, Giuseppe Serra, and Rita Cucchiara. A deep multi-level network for saliency prediction. In *2016 23rd International Conference on Pattern Recognition (ICPR)*, pages 3488–3493. IEEE, 2016. 8, 15, 16
47. Pengfei Wang, Chengquan Zhang, Fei Qi, Shanshan Liu, Xiaoqiang Zhang, Pengyuan Lyu, Junyu Han, Jingtuo Liu, Errui Ding, and Guangming Shi. Pgnnet: Real-time arbitrarily-shaped text spotting with point gathering network. In *Proceedings of the AAAI Conference on Artificial Intelligence*, volume 35, pages 2782–2790, 2021. 8, 15, 16

## A Experimental Settings

### A.1 Implementation Details.

For the four datasets, we followed the data processing rules in [38]. The video split rule followed the original datasets for a fair comparison. The initialized learning rate of 0.01 decayed as the exponential equation by a constant of 0.8 after every epoch. Stochastic Gradient Descent with the momentum of 0.9 and weight decay of  $10^{-4}$  was employed to optimize the network. We froze the weight of the Swin transformer trained on the ImageNet dataset. Batch size was set to 4 for all datasets. We set the joint training iterations to 16 epochs for all datasets. The model training was stopped as soon as the performance on the DADA validation set consecutively decreased three times than the performance at the prior training epoch. Our model was implemented using the PyTorch framework and trained on two NVIDIA A800 GPUs.

### A.2 Datasets.

Our proposed AHMF model was jointly trained on four available driver attention datasets, *i.e.*, BDD-A [17], DADA [41], DReyeVE [42], and EyeTrack [19]. The Berkeley DeepDrive attention (BDD-A) dataset was filtered from the BDDV dataset, focusing on braking events in heavy traffic. Forty-five gaze providers labeled 1,429 critical scene videos. The Driver Attention and Driver Accident (DADA) dataset includes 2,000 accident videos across 54 kinds of accident scenarios collected from public websites worldwide. Twenty volunteers annotated visual attention points using the infrared eye tracker under lab conditions. DReyeVE was the first large-scale public driver attention dataset, comprising 74 traffic video clips collected from naturalistic driving experiments. EyeTrack’s traffic videos were collected by a dashcam on urban highways in China, and gaze data were captured in-lab as 28 subjects viewed the recorded clips.

### A.3 Evaluation Metrics.

To comprehensively evaluate the performance of our proposed method, we adopt various saliency evaluation metrics, including three distribution-based metrics, *i.e.*, Similarity (SIM), Kullback-Leibler divergence (KLD), and Pearson’s correlation coefficient (CC), and two location-based metrics, *i.e.*, Normalized Scanpath Saliency (NSS) and Area Under ROC Curve Judd (AUC-J), calculated as:

$$KLD(S, \hat{S}) = \sum_{i=1}^N S(i) \log \left( \varepsilon + \frac{S(i)}{\varepsilon + \hat{S}(i)} \right) \quad (5)$$

$$CC(S, \hat{S}) = \frac{\text{cov}(S, \hat{S})}{\sigma(S) \cdot \sigma(\hat{S})} \quad (6)$$

$$\text{SIM}(S, \hat{S}) = \sum_{i=1}^N \min(S(i), \hat{S}(i)) \quad (7)$$

$$NSS(P, \hat{S}) = \frac{1}{\sum_{i=1}^N P_i} \times \sum_{i=1}^N P_i \frac{\hat{S} - \mu_{\hat{S}}}{\sigma_{\hat{S}}} \quad (8)$$

where  $S$  and  $\hat{S}$  are the ground-truth and predicted saliency maps, respectively,  $P$  is the ground-truth fixation point map, index  $i$  denotes the  $i$ -th pixel across all  $N$  pixels.

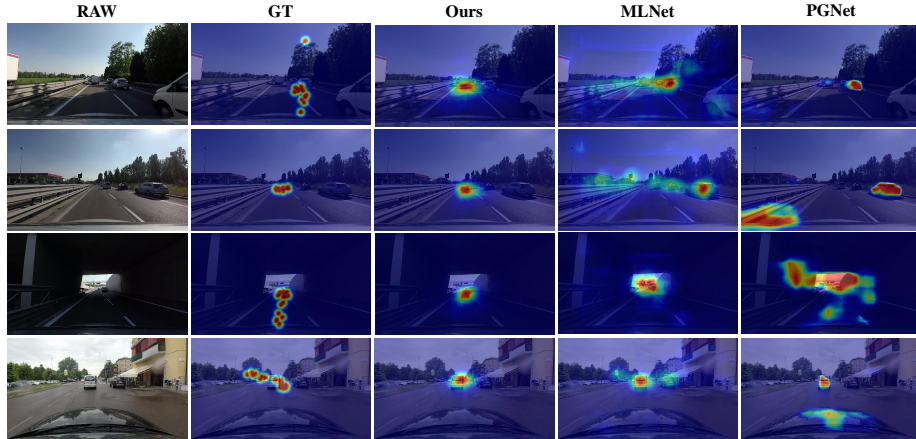


**Fig. 3:** Qualitative results of the predicted driver attention maps in the DREyeVE dataset. From left to right: raw inputs, ground-truth attention maps, predictions of ours, MLNet [46], and PGNet [47].

## B Results

### B.1 Qualitative Results

As illustrated in Figure 3, the qualitative results demonstrate the superiority of our method when tested on the DREyeVE dataset. In the video frame sequence tests on highways, the MLNet model tends to disperse part of its attention to stationary vehicles in adjacent lanes, whereas human drivers primarily focus their attention on the road ahead. Similarly, the PGNet model not only disperses attention but also fails to handle vehicle reflections adequately, leading to an excessive focus on the host vehicle. Additionally, PGNet performs poorly in scenarios with contrasting lighting conditions, such as tunnels. In contrast, our model more accurately simulates human attention distribution, with its attention prediction results being highly consistent with the ground truth.

The results in Figure 4 illustrate the comparative performance of our proposed method against several baseline approaches on the BDD-A dataset. Notably, MLNet’s attention distribution frequently targets vehicles or objects situated outside the driving lane. In scenarios devoid of prominent vehicles, both



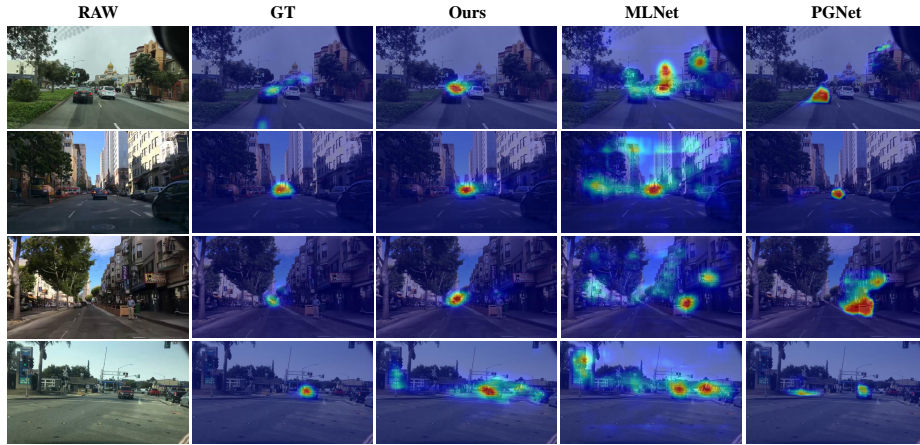


**Fig. 4:** Qualitative results of the predicted driver attention maps in the BDD-A dataset. From left to right: raw inputs, ground-truth attention maps, predictions of ours, MLNet [46], and PGNet [47].

MLNet and PGNet exhibit a propensity to divert their attention towards roadside objects. Conversely, our model more accurately replicates human attention distribution, with its predicted attention maps exhibiting a high degree of congruence with the ground truth. These findings underscore the superior capability of our model to emulate driver attention, demonstrating enhanced focus on regions pertinent to the driving task.

**Table 4:** Ablation study for different components of AHMF on DADA and BDD-A dataset.

Method	DADA [41]					BDD-A [17]				
	AUC-J $\uparrow$	SIM $\uparrow$	CC $\uparrow$	KLD $\downarrow$	NSS $\uparrow$	AUC-J $\uparrow$	SIM $\uparrow$	CC $\uparrow$	KLD $\downarrow$	NSS $\uparrow$
<b>AHMF</b>	<b>0.94</b>	<b>0.57</b>	<b>0.50</b>	<b>1.55</b>	<b>5.02</b>	<b>0.92</b>	<b>0.75</b>	<b>0.58</b>	<b>1.17</b>	<b>5.51</b>
-SA	0.92	0.56	0.49	1.56	4.95	0.91	0.75	0.57	1.21	5.43
-CA	0.93	0.53	0.48	1.56	4.83	0.91	0.75	0.56	1.20	5.44
-HMF	0.92	0.44	0.47	1.61	4.49	0.91	0.61	0.57	1.19	4.94

**Table 5:** Ablation study for the position of the accumulation long-term memories.

Location	DADA [41]					BDD-A [17]				
	AUC-J $\uparrow$	SIM $\uparrow$	CC $\uparrow$	KLD $\downarrow$	NSS $\uparrow$	AUC-J $\uparrow$	SIM $\uparrow$	CC $\uparrow$	KLD $\downarrow$	NSS $\uparrow$
After HMF	<b>0.94</b>	<b>0.57</b>	<b>0.50</b>	<b>1.55</b>	<b>5.02</b>	<b>0.92</b>	<b>0.75</b>	<b>0.58</b>	1.17	<b>5.51</b>
After CA	0.92	0.54	0.49	<b>1.55</b>	4.98	0.91	0.72	<b>0.58</b>	<b>1.16</b>	5.36

**Table 6:** Ablation study for backbones. SWT represents Swin-Transformer-Tiny.

Method	Paras	FLOPS	DADA [41]					BDD-A [17]				
			AUC-J $\uparrow$	SIM $\uparrow$	CC $\uparrow$	KLD $\downarrow$	NSS $\uparrow$	AUC-J $\uparrow$	SIM $\uparrow$	CC $\uparrow$	KLD $\downarrow$	NSS $\uparrow$
SWT	28.2M	4.38G	<b>0.94</b>	<b>0.57</b>	<b>0.50</b>	<b>1.55</b>	<b>5.02</b>	<b>0.92</b>	<b>0.75</b>	<b>0.58</b>	<b>1.17</b>	<b>5.51</b>
Resnet-50	25.6M	4.13G	0.92	0.52	0.47	1.60	4.76	0.91	0.73	<b>0.58</b>	1.18	5.43

## B.2 Ablation Study

Table 4 presents the results of an ablation study evaluating the contributions of different components of AHMF on the DADA and BDD-A datasets. The full AHMF model is compared against three variants: without the Self-Attention (SA) module, without the Channel-Attention (CA) module, and without the Hybrid-Memory-Fusion (HMF) module. The results on both datasets indicate that each component contributes to the model’s effectiveness, with the combination of all components yielding the optimal performance. Among the three core components, removing the HMF module causes the most significant performance degradation, reducing NSS by -10.6% and -10.3% on the DADA and

**Table 7:** Ablation study on the length of historical input sequences.

Length	DADA [41]					BDD-A [17]				
	AUC-J $\uparrow$	SIM $\uparrow$	CC $\uparrow$	KLD $\downarrow$	NSS $\uparrow$	AUC-J $\uparrow$	SIM $\uparrow$	CC $\uparrow$	KLD $\downarrow$	NSS $\uparrow$
30	<b>0.94</b>	<b>0.57</b>	<b>0.50</b>	<b>1.55</b>	<b>5.02</b>	<b>0.92</b>	0.75	<b>0.58</b>	1.17	<b>5.51</b>
20	0.92	<b>0.57</b>	0.47	1.58	4.81	0.91	0.75	<b>0.58</b>	1.14	5.42
15	0.92	0.55	0.48	<b>1.55</b>	4.86	0.91	0.73	0.57	<b>1.12</b>	5.47
10	0.92	0.53	0.48	1.57	4.79	0.91	0.72	<b>0.58</b>	1.14	5.37
5	0.92	0.56	0.47	1.60	4.65	0.91	<b>0.79</b>	0.57	1.23	5.35

BDD-A datasets, respectively. This demonstrates the importance of introducing the long-term memory module and designing an appropriate hybrid memory fusion module for driver attention prediction tasks.

Table 5 displays an ablation study for the position of the long-term memory updating module. The results show that updating long-term memories after the HMF module results in slightly better performance across most metrics compared to updating it after CA. This discrepancy can be attributed to the nature of the feature information processing in these stages. After the HMF phase, the amalgamation of feature information enables the model to more effectively leverage memory, thereby optimizing performance. Conversely, after the CA module, the feature information tends to become more abstract and hierarchical, potentially disrupting the initial memory sequence and leading to a drop in performance.

Table 6 demonstrates that using Swin-Transformer-Tiny (SWT) as the backbone outperforms Resnet-50 on both the DADA and BDD-A datasets.

The ablation study in Table 7 shows that using longer historical input sequences significantly enhances model performance across various metrics for both the DADA and BDD-A datasets. The highest AUC-J, SIM, and NSS scores are achieved with a length of 30, indicating that capturing more temporal information allows the model to better encode working memories to fully understand current traffic scenarios and potentially conflicting objects. Additionally, longer sequences also reduce noise and contribute to more robust predictions.